Pressure-induced polymorphism in cyclopropylamine

Patricia Lozano-Casal,* David R. Allan and Simon Parsons

School of Chemistry, The University of Edinburgh, West Mains Road, Edinburgh EH9 3JJ, Scotland

Correspondence e-mail:
p.lozano-casal@ed.ac.uk

The crystal structure of cyclopropylamine at 1.2 GPa has been determined by X-ray diffraction methods. The structure of this phase is orthorhombic, space group *Pbca* and the unit-cell dimensions are $a = 5.0741$ (10), $b = 9.7594$ (10) and $c = 13.305$ (2) Å. Only one of the two H atoms of the amino group actively participates in the formation of the hydrogen-bonded chains, $C(2)$ in graph-set notation, which lie parallel to the crystallographic *a* axis. Additionally, the topology of the crystal packing is studied using both Voronoi–Dirichlet polyhedra and Hirshfeld surface analyses for the low-temperature and the high-pressure structures of cyclopropylamine and the results are compared.

1. Introduction

The main features of the hydrogen bond, which determine its strength, are the donor H atom to acceptor distance and the angle formed between them. The strength of the hydrogen bond increases as the donor H atom to acceptor distance decreases and as the angle donor—H atom—acceptor gets closer to 180°. The electronegative character of the donor and acceptor atoms plays an important role in the strength of hydrogen bonding. Thus, the more electronegative the atoms, the stronger the hydrogen bond. Typical distances for strong hydrogen bonds are between 1.2 and 1.5 Å, with angles between 170 and 180° and an example of such a bond is F—H···F. However, the type of hydrogen bond reported in this work is the N—H···N hydrogen bond, which is classified as moderate to weak (Desiraju & Steiner, 2001; Steiner, 2002), with distances between 1.5 and 2.2 Å, and angles greater than 130°. This type of hydrogen bond is commonly present in amines and their derivatives, and it is present in cyclopropylamine. Pressure has a significant effect not only on the hydrogen bond but on other intermolecular interactions present in the crystal structure such as van der Waals forces and steric effects. Consequently, when pressure is applied to the structure, the molecules are displaced from their equilibrium positions to form a generally more compact packing. These changes are driven by the competition between the formation of hydrogen bonding, minimizing steric effects and the necessity of achieving a maximum coordination index, and an optimum filling of space. Hydrogen-bond distances are, consequently, compressed (or expanded) as a consequence of pressure. Therefore, the study of how the properties of the hydrogen bonding are influenced by pressure might enhance our understanding of the hydrogen bond and, in turn, the crystal structures that these molecular systems adopt.

Table 1
Experimental details for the data collection of cyclopropylamine at 12 GPa.

Crystal data	
Chemical formula	C_3H_7N
M_r	57.10
Cell setting, space group	Orthorhombic, $Pbca$
a, b, c (Å)	5.0741 (10), 9.7594 (10), 13.305 (2)
α, β, γ (°)	90.00, 90.00, 90.00
V (Å³)	658.89 (19)
Z	8
D_x (Mg m⁻³)	1.151
Radiation type	Mo $K\alpha$
No. of reflections for cell parameters	844
θ range (°)	2.6–23.0
μ (mm⁻¹)	0.07
Temperature (K)	293 (2)
Crystal form, colour	Block, colourless
Crystal size (mm)	Not measured
Data collection	
Diffractometer	CCD area detector
Data collection method	ω scans
Absorption correction	Multiscan (based on symmetry-related measurements)
T_{min}	0.799
T_{max}	1.000
No. of measured, independent and observed reflections	371, 371, 344
Criterion for observed reflections	$I > 2\sigma(I)$
R_{int}	0.065
θ_{max} (°)	23.3
Range of h, k, l	$-4 \Rightarrow h \Rightarrow 4$
	$-10 \Rightarrow k \Rightarrow 10$
	$-13 \Rightarrow l \Rightarrow 13$
Refinement	
Refinement on	F^2
$R[F^2 > 2\sigma(F^2)], wR(F^2), S$	0.042, 0.096, 1.18
No. of reflections	371
No. of parameters	65
H-atom treatment	Mixture of independent and constrained refinement
Weighting scheme	$w = 1/[\sigma^2(F_o^2) + (0.0403P)^2 + 0.229P]$, where $P = (F_o^2 + 2F_c^2)/3$
$(\Delta/\sigma)_{max}$	<0.0001
$\Delta\rho_{max}, \Delta\rho_{min}$ (e Å⁻³)	0.11, −0.14

Computer programs used: *SMART* (Bruker-AXS, 1997–2001), *SHELXTL* (Sheldrick, 1997a), *SHELXS97* (Sheldrick, 1997b), *SHELXL97* (Sheldrick, 1997c).

As well as inducing changes in the geometry of intermolecular interactions, pressure can also affect the crystal structures of small-molecule systems leading to the formation of previously unobserved polymorphs. We have already investigated the high-pressure polymorphism of a range of fundamental small-molecule systems including simple mono-alcohols and carboxylic acids (for example, methanol, ethanol, formic acid, acetic acid and propionic acid), ketones (such as acetone) and the oxoacids (such as sulfuric acid; Allan *et al.*, 1998; Allan & Clark, 1999*a,b*; Allan *et al.*, 1999, 2000, 2001, 2002). We have also investigated more complex molecular materials such as pharmaceutical compounds [*e.g.* para-cetamol (Fabbiani *et al.*, 2003)].

We are now extending this work to include other monofunctional systems, such as the amines, and here we report a high-pressure polymorph of cyclopropylamine, whose structure has been determined at 1.2 GPa using single-crystal X-ray

diffraction techniques. The new phase, phase II, crystallizes at high pressure in the orthorhombic space group *Pbca*, with one molecule in the asymmetric unit and eight molecules in the unit cell. The previously reported low-temperature phase I structure crystallizes in the rhombohedral space group *R3c*. A detailed analysis and comparison of the hydrogen bonding in both polymorphs reveals substantial differences. The molecules at high pressure are no longer arranged in $R_3^3(6)$ rings but, instead, they form zigzag chains of molecules along the *a* axis, expressed as $C(2)$ in the graph-set notation (Berstein *et al.*, 1995).

2. Experimental

Liquid cyclopropylamine was loaded and pressurized in a Merrill–Bassett diamond–anvil cell (DAC; Merrill & Basset, 1974) that was equipped with 600 μm culet diamonds and a tungsten gasket. After the nucleation of several crystallites on pressure increase, the temperature was cycled close to the melting point in order to reduce the number of crystallites until only one crystallite remained. Finally, a single crystal was obtained at 1.2 GPa, after the cell was allowed to cool to ambient temperature.

The DAC was then mounted and centred on a Bruker SMART APEX diffractometer (graphite-monochromated Mo $K\alpha$ radiation) and a sequence of eight data-collection scans was initiated, following the data-collection strategy of Dawson *et al.* (2004). The *SMART* program (Bruker-AXS, 1997–2001, 1999) was used for data-collection control and, with a detector distance of 70 mm, 2θ was set at either +28° or −28° to provide maximum coverage. No beam stop was used as, with this selection of detector distance and 2θ, the primary beam does not impinge on the detector aperture. The eight scans were conducted as a sequence of 3σ frames that each had a range of 0.3° in ω and an exposure time of 30 s. The φ axis was fixed at either 90 or 270°, to ensure that the axis of the diamond-anvil cell was held parallel to the $\omega/2\theta$ plane so that absorption from the pressure-cell components was minimized and the maximum possible access of reciprocal space was achieved. The overall data-collection time was 15 h. The sample reflections were identified by hand with the aid of the *SMART* code, and an orientation matrix was determined using the *GEMINI* program (Bruker-AXS, 1999). Data integration and global-cell refinement were performed with the program *SAINT* (Bruker-AXS, 2002). The program *ABSORB* (Angel, 2004) was used to apply a correction for the absorption caused by the DAC and gasket 'shadowing', rejecting reflections for which either the incident or the diffracted beam were completely absorbed by the cell and resulted in shading of the detector. The remaining reflections were corrected for any residual absorption by the pressure-cell components with the program *SORTAV* (Blessing, 1995, 1997) and the transmission ranged from 1.017 to 1.273.

The structure was solved in *Pbca* using direct methods (*SHELXTL*; Sheldrick, 1997a) and subsequently refined against F^2. The crystal structure is composed of eight molecules in the unit cell with one in the asymmetric unit. The
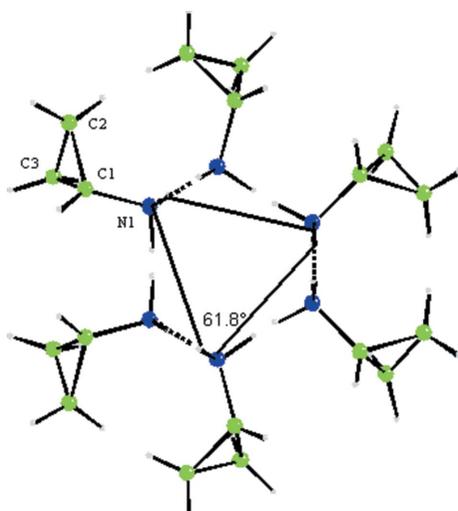
Table 2
Selected hydrogen-bond distances (Å) and bond angles (°) for the high-pressure phase II of cyclopropylamine from the experimental studies at 12 GPa and for the low-temperature phase I of cyclopropylamine taken from the reported structure by de Boer *et al.* (1986).

Interaction	N—H···N (Å)	N···N (Å)	N—H···N (°)	N···N—C (°)
Phase II				
N—H7···N[i]	2.30 (3)	3.166 (3)	167 (2)	117.5
Phase I				
N—H6···N[ii]	2.711	3.541	150	130
N—H7···N[iii]	2.285	3.230	177	111

Symmetry codes: (i) $-\frac{1}{2}+x, y, \frac{1}{2}-z$; (ii) $-x+y, -x, z$; (iii) $x, x-y, -\frac{1}{2}+z$.

unit-cell parameters are a = 5.0741 (10), b = 9.7594 (10) and c = 13.305 (2) Å at 1.2 GPa. One of the most serious difficulties encountered in high-pressure crystallography is the limited volume of reciprocal space that can be sampled owing to shading by the body of the pressure cell. For the Merrill–Basset cell used in this study, the volume of accessible reciprocal space is limited to approximately 40% of what would be expected for a sample collected on a fibre at ambient conditions to the same resolution. However, the completeness of the data set collected here is 77.9% to 2θ = 46.5°, despite the constraints of the pressure cell, owing to the relatively high symmetry of the *Pbca* space group and the orientation of the crystal within the cell. All the H atoms were found in the difference map. A full anisotropic refinement with independent positional parameters for each atom was performed and a common isotropic displacement parameter was also modelled for the H atoms. The structure refined to R = 0.042, R_w = 0.096 for 65 parameters and 344 data with $F > 2\sigma(F)$. The final difference map extremes were 0.114 and -0.138 e Å^{-3} and the

goodness of fit was 1.176. The refinement and experimental details are presented in Table 1.[1]

3. Discussion

3.1. Low-temperature structure (phase I)

Although the low-temperature structure of cyclopropylamine has already been reported (de Boer *et al.*, 1986; CSD refcode FIGYID), a complete description has not been given of how the molecules are arranged in the crystal structure or the hydrogen bonding. It is important, therefore, to describe the structure at low temperature in detail, in order to compare it to the crystal structure determined at high pressure.

Phase I of cyclopropylamine crystallizes at 170.5 K in the rhombohedral space group *R3c*, with 18 molecules in the unit cell and one in the asymmetric unit. The hexagonal unit-cell parameters are a = 18.784 (2) and c = 5.494 (2) Å. The C atoms of the molecule lie in the same plane, parallel to $\{1\bar{7}\bar{1}\}$ and the N atom is rotated out of this plane by 147.3° with respect to the C atoms. There are two different N—H···N hydrogen-bond interactions (Table 2) present in the structure, which are formed by each of the two H atoms in the amino group. What appear to be very long, and therefore very weak, N—H6···N interactions form three-membered rings, or trimers, stacked along the crystallographic c axis, with alternate trimers rotated by 61.8° (see Figs. 1 and 2). This contact would be defined as $R_3^3(6)$ in graph-set notation, as the three-membered rings are apparently formed by three donors and three acceptors. However, the distance of this interaction is significantly longer, by ~ 0.2 Å, than the normal range for N···N hydrogen bonds and, although the N—H6···N bond angle (150°) would be within expected limits, it is unlikely to offer a significant contribution to the overall intermolecular bonding in the structure. The trimers are bridged by shorter N—H7···N hydrogen bonds, which form $C(2)$ zigzag chains of molecules along the crystallographic c direction (Fig. 3).

An alternative way of describing the crystal structure is by examining an individual molecule and its neighbouring environment. By doing so, an octahedron is formed by molecules and their closest neighbours (Fig. 4). Each polyhedron is formed by six molecules and the N atom of each of the molecules has a nearest N atom at a distance of 3.230 Å, a pair of N atoms at 3.541 Å and a single N atom at 3.629 Å. The octahedra are coupled to form infinite columns along the crystallographic c direction where each of the octahedra share one face and follow an alternating sequence of parallel and perpendicular octahedra, with respect to their axial directions. Overall, each molecule is coordinated by 14 nearest neighbours.

3.2. High-pressure structure (phase II)

At 1.2 GPa, the N atom is rotated 148.7° out of the plane formed by the atoms C1, C2 and C3, which form the ring of C

Figure 1
A view along the hydrogen-bond pattern formed by two coupled $R_3^3(6)$ trimers in the low-temperature phase I of cyclopropylamine (de Boer *et al.*, 1986). The trimers are formed by long N—H6···N interactions (shown by the solid lines) and alternate trimers are rotated by 61.8° with respect to its neighbours. The trimers are bridged by shorter N—H7···N hydrogen bonds.

atoms. The cyclopropylamine phase II structure at high pressure is simply formed by molecules connected in a zigzag pattern, *via* a *cis*-N—H$\cdots$N hydrogen bond, forming sets of infinite chains [N$\cdots$N distance 3.166 (3) Å], expressed as *C*(2) in graph-set notation (the repeating unit contains one hydrogen-bond donor and one acceptor). These chains lie parallel to the crystallographic *a* axis, as can be seen from Figs. 5 and 6. Only one of the two H atoms, H7, from the amino group participates in the hydrogen bonding. All the molecules of cyclopropylamine lie on the same side of the plane formed by the chain of hydrogen bonds (Fig. 5). From the view looking down the hydrogen bond (N—H$\cdots$N), the dihedral

angle formed by the atoms involved in its formation (C—N—N—C) is 71°, which is relatively close to the 60° required for an ideal *gauche* conformation. Details about the distances and angles of the hydrogen bond can be found in Table 2.

The packing motifs adopted by monoalcohols, *R*OH (Brock & Duncan, 1994), arise from a compromise between the packing requirements of the relatively bulky *R* groups present in the molecules and the necessity of the hydroxyl groups to get close enough to form the hydrogen bonding. If the *R* groups are relatively small, the molecules containing the
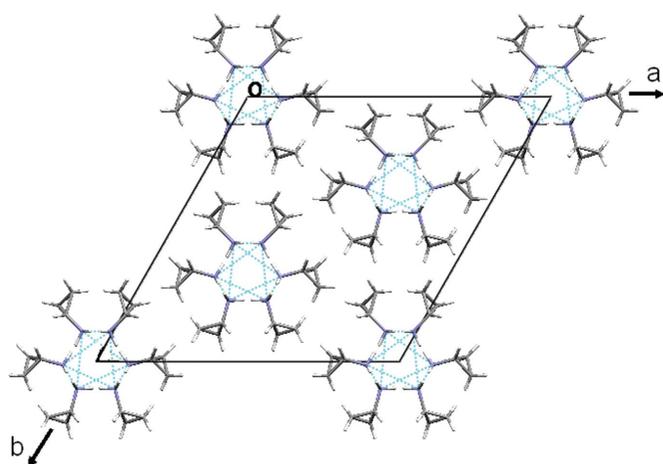

Figure 2
Projection down the crystallographic *c* axis of the low-temperature phase I crystal structure of cyclopropylamine (de Boer *et al.*, 1986).
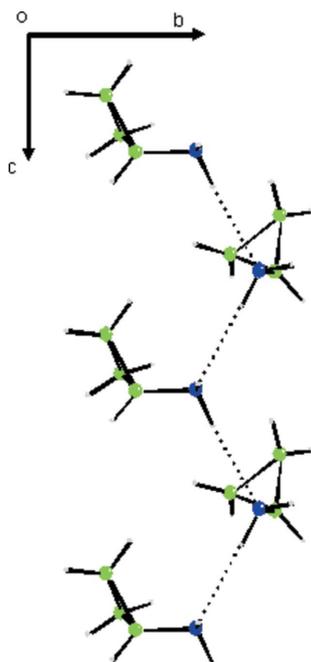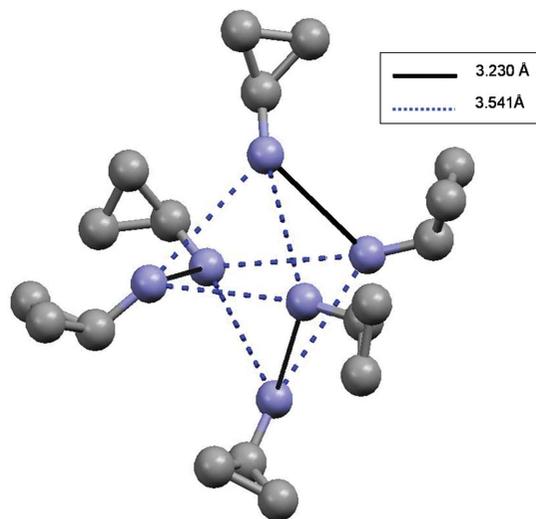

Figure 4
Octahedron formed by the arrangement of molecules linked by the N—H$\cdots$N hydrogen bond and the weak N—H$\cdots$N contact in the low-temperature phase of cyclopropylamine (de Boer *et al.*, 1986). Only the non-H atoms are shown. The bond distances (edges) of the polyhedron are displayed. The long (3.629 Å) N$\cdots$N contact is omitted.

Figure 3
A view of the *C*(2) chains, formed by the N–H7$\cdots$N hydrogen bond, which run parallel to the *c*-axis direction in the low-temperature phase I crystal structure of cyclopropylamine (de Boer *et al.*, 1986).
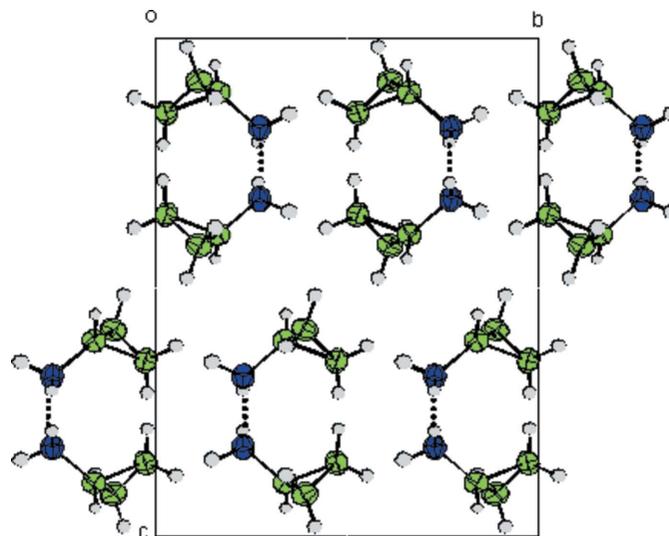

Figure 5
An *a*-axis projection of the high-pressure, *Pbca*, structure of cyclopropylamine at 1.2 GPa. The crystallographic *b* axis is horizontal while the *c* axis is vertical. The molecules are linked *via cis* hydrogen bonds.

hydroxyl groups will be related by translational symmetry (glide plane or 2_1 screw axis) forming an approximately coplanar alternating sequence about the central hydrogen-bonded core. For bulkier R groups, the molecules often cannot adopt a simple arrangement owing to steric effects and instead they form chains along three-, four- and sixfold screw axes. Finally, if the R groups occupy an even greater volume, cyclic dimer, trimer, tetramer or hexamer rings can be formed.

Thus, the structures of the two cyclopropylamine polymorphs can be compared with the structures of the mono-alcohols at both low temperature and high pressure, which, in general, form molecular chains differing in the arrangement of the molecules about the chains. For example, the crystal structure of ethanol at ambient pressure (Jönsson, 1976) forms infinite chains where the molecules are connected by *cis*- and *trans*-O—H···O hydrogen bonds. However, at high pressure, the molecules of ethanol form linear hydrogen-bonded chains, where the molecules are linked in each chain with their methyl groups aligned in the same direction along the *b* axis (Allan & Clark, 1999*a*; Allan *et al.*, 2001). Other similar cases are the low-temperature and high-pressure polymorphs of methanol (Tauer & Lipscomb, 1952; Narten & Habenschuss, 1984; Torrie *et al.*, 1989; Allan *et al.*, 1998), cyclobutanol (McGregor *et al.*, 2005) and phenol and mono-fluorophenols, such as 2-chlorophenol and 4-fluorophenol (Oswald *et al.*, 2005). All the mono-fluorophenols as well as phenol and cyclopropylamine crystallize under pressure in low-symmetry space groups with the molecules disposed about 2_1 screw axes. Thus, cyclopropylamine presents a polymorphism similar to that found in alcohols, where pseudo-helices and ring motifs are often observed at low temperature. However, at high pressure they tend to form hydrogen-bonded chains with a simple alternating sequence.
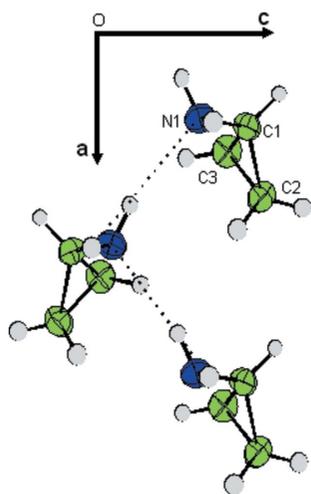
3.3. Comparison of the low-temperature phase I and high-pressure phase II crystal structures

3.3.1. Hirshfeld surfaces. The program *Crystal Explorer* (UWA Theoretical Chemistry, undated) makes use of Hirshfeld surfaces to partition crystal space in molecular crystals so that the packing modes and intermolecular interactions can be explored (McKinnon *et al.*, 2004). We have used this program to visualize the packing behaviour in phase I and phase II of cyclopropylamine in order to make a more detailed comparison between them.

Hirshfeld surfaces (Hirshfeld, 1977) for the low-temperature and high-pressure polymorphs of cyclopropylamine are shown in Fig. 7, with the H atoms of the amino group at the top pointing away from the viewer in each case. Only one of the two H atoms of the amino group in the high-pressure phase II polymorph actively participates in the hydrogen bond. This is shown by the red–orange region on the d_e surface adjacent to the N atom (where d_e is the distance to the nearest atom centre exterior to the surface). This situation is also observed in the even members of the diamines (*e.g.* 1,2-ethanediamine, 1,4-butanediamine, 1,6-hexanediamine), as was explained by McKinnon *et al.* (2004). Hirshfeld surfaces for the high-pressure polymorph show that there is clearly only a single interaction that could be classified as a hydrogen bond (interaction 1 in Fig. 7). However, the Hirshfeld surfaces for the low-temperature polymorph show a strong contact and a weak contact (interactions 1 and 2 in Fig. 7) present in the structure,
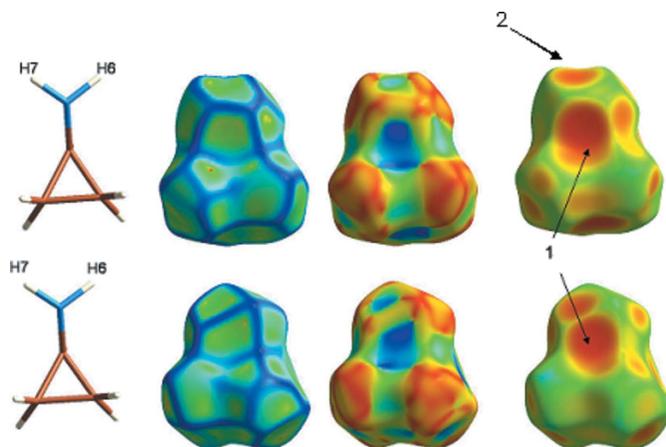

Figure 6
One of the crystallographically $C(2)$ unique hydrogen-bonded chains in cyclopropylamine at 1.2 GPa viewed along the *b* axis. The molecules adopt an alternating 1–1–1 sequence.

Figure 7
Hirshfeld surfaces for the low-temperature phase I (top) and high-pressure phase II (bottom) polymorphs of cyclopropylamine. Each molecule is shown with the Hirshfeld surface mapped with curvedness (left), shape index (centre) and d_e (right), which is the distance to the nearest atom centre exterior to the surface [for this series mapped between 1.0 Å (red) and 2.5 Å (blue)]. The labels 1 and 2 correspond to the strong and weak hydrogen-bond interactions, respectively, present in the crystal structures of phase I and phase II. The NH$_2$ group of the cyclopropylamine molecule for both these projections is oriented in the same way for phase I and phase II with the N atom pointing towards the viewer and the H atoms pointing away from the viewer (as can be seen from the sketch of the molecule shown beside the Hirshfeld surfaces). The H7 and H6 atoms of the low-temperature phase I are involved in the formation of a short and a long hydrogen bond, respectively, whereas the H7 atom of the high-pressure phase II is the only H atom that participates in the formation of hydrogen bonding.

which is common to the odd members of the diamines (*e.g.* 1,3-propanediamine and 1,5-pentanediamine).

The two-dimensional fingerprint plots (plot of d_i versus d_e, where d_i is the distance to the nearest atom centre interior to the surface) for the two polymorphs stress the systematic differences between the two structures (Fig. 8). One of the main differences is that the voids (upper region of the plots in Fig. 8) are more compact in the high-pressure phase II crystal structure than in the low-temperature phase I structure, indicating that the packing is more efficient. The second difference is that both structures present relatively short hydrogen bonds (the distances labelled 1 in Fig. 8), one of which is slightly shorter in the case of the phase II polymorph. Finally, the phase I structure has two significant hydrogen bonds, while the high-pressure structure has only the one, short, hydrogen bond with the remaining amino H atom not involved in bonding. It can be seen that the second, longer, hydrogen bond of the low-temperature phase I polymorph is weak in nature as it does not form part of the sharp spikes in the Hirshfeld fingerprint, which represent the strong hydrogen bonds (the distance labelled 2 in Fig. 8).
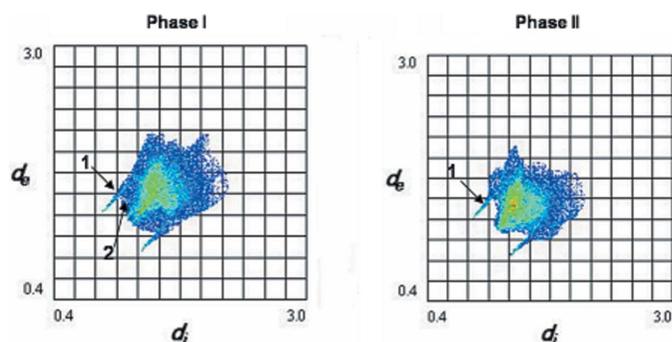

Figure 8
Two-dimensional fingerprint plots for the low-temperature (left) and high-pressure (right) polymorphs of cyclopropylamine. The labels 1 and 2 correspond to the strong and weak hydrogen-bond interactions, respectively, present in the crystal structures of phase I and phase II. d_e and d_i are the distances to the nearest atom centre exterior and interior to the surface, respectively.
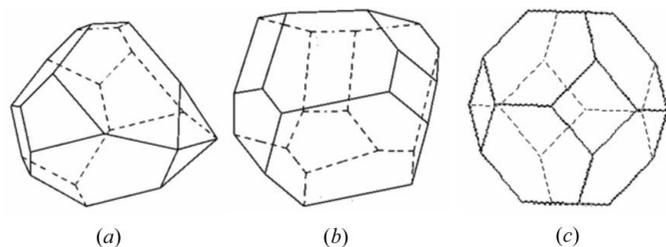

Figure 9
Lattice Voronoi–Dirichlet polyhedra in: (*a*) the low-temperature polymorph and (*b*) the high-pressure polymorph of cyclopropylamine and (*c*) for perfect body-centred cubic packing. Combinatorial types (Peresypkina & Blatov, 2000) can be written as $f/v - n$, where f is the number of faces and v is the number of vertices; n is just an ordinal number to distinguish different VDPs where f and v are equal. These are: (*a*) 14/21–1, (*b*) 14/24–1 and (*c*) 14/24–1. The combinatorial types for (*b*) and (*c*) are therefore equivalent.

3.3.2. Topological analysis. Topological analyses of phase I and phase II can be useful to rationalize the more significant structural changes caused by pressure. Voronoi–Dirichlet polyhedra (VDPs) were used to analyse the molecular structure of the two polymorphs of cyclopropylamine (Blatov, 2004).

The calculation of molecular coordination numbers, and topological and geometrical analysis of the environment of the two different polymorphs of cyclopropylamine were carried out by using the *TOPOS4.0* program suite (Blatov *et al.*, 1999). Adjacent matrices were calculated using the *AUTOCN* program using the method of spherical sectors; the minimum solid angle of a Voronoi–Dirichlet polyhedron (VDP) face corresponding to an intermolecular contact was set to zero. Analyses of the VDPs were carried out with the program *ADS*, with the geometrical centres of the molecules (as opposed to their centres of gravity) as reference points. Coordination sequences were calculated out to three coordination spheres. The results of the topological analysis of cyclopropylamine polymorphs are presented in Fig. 9. The coordination sequences are 14–54–122 and 14–53–120 for the phase I and phase II crystal structures, respectively. Consequently, it can be seen that the structure of phase II is closer to a perfect body-centred cubic structure (14–50–110) than that of phase I. Nevertheless, both structures are significantly distorted from body-centred cubic.

4. Conclusions

We have determined the high-pressure crystal structure of cyclopropylamine at 1.2 GPa. All the atomic positions were found, including those of the H atoms. Therefore, as the H-atom positions were determined completely, it can be demonstrated directly, and without resorting to purely geometrical considerations, that only one of the H atoms of the amino group is involved in the hydrogen bonding. As both H atoms appear to be involved in the hydrogen bonding in the crystal structure of phase I, this represents a significant difference between the two polymorphs. This change in bonding was also observed in the differences between the Hirshfeld surfaces and fingerprint plots for the two different polymorphs of cyclopropylamine. Finally, the molecular packing environments were studied for the low-temperature and the high-pressure phases I and II of cyclopropylamine and compared with that for perfect body-centred cubic. The molecular environment at 1.2 GPa was found to be less distorted from ideal body-centred cubic packing than that at low temperature.

References

Allan, D. R . & Clark, S. J. (1999*a*). *J. Phys. Rev. B*, **60**, 6328–6334.
Allan, D. R. & Clark, S. J. (1999*b*). *J. Phys. Rev. Lett.* **82**, 3464–3467.

Allan, D. R., Clark, S. J., Brugmans, M. J. P., Ackland, G. J. & Vos, W. L. (1998). *Phys. Rev. B*, **58**, R11809.

Allan, D. R., Clark, S. J., Dawson, A., McGregor, P. A. & Parsons, S. (2002). *Acta Cryst.* B**58**, 1018–1024.

Allan, D. R., Clark, S. J., Ibberson, R. M., Parsons, S., Pulham, C. R. & Sawyer, L. (1999). *Chem. Commun.* **8**, 751–752.

Allan, D. R., Clark, S. J., Parsons, S. & Ruf, M. (2000). *J. Phys. Condens. Matter*, **12**, L613–L618.

Allan, D. R., Parsons, S. & Teat, S. J. (2001). *J. Synchrotron Rad.* **8**, 10–17.

Angel, R. J. (2004). *J. Appl. Cryst.* **37**, 486–492.

Berstein, J., Davis, R. E., Shimoni, L. & Chang, N. L. (1995). *Angew. Chem. Int. Ed. Engl.* **34**, 1555–1573.

Blatov, V. A. (2004). *Crystallogr. Rev.* **10**, 249–318.

Blatov, V. A., Shevchenko, A. P. & Serezhkin, V. N. (1999). *Russ. J. Coord. Chem.* **25**, 453–465.

Blessing, R. H. (1995). *Acta Cryst.* A**51**, 33–38.

Blessing, R. H. (1997). *J. Appl. Cryst.* **30**, 421–426.

Boer, J. S. A. M. de, Schenk, H. & Stam, C. H. (1986). *Rec. Trav. Chim.* **105**, 434–435.

Brock, C. P. & Duncan, L. L. (1994). *Chem. Mater.* **6**, 1307–1312.

Bruker-AXS (1997–2001). *SMART*, Version 5.049–5.059. Bruker-AXS, Madison, Wisconsin, USA.

Bruker-AXS (1999). *GEMINI*, Version 1.01. Bruker-AXS, Madison, Wisconsin, USA.

Bruker-AXS (2002). *SAINT*, Version 6. Bruker-AXS, Madison, Wisconsin, USA.

Dawson, A., Allan, D. R., Parsons, S. & Ruf, M. (2004). *J. Appl. Cryst.* **37**, 410–416.

Desiraju, G. & Steiner, T. (2001). *The Weak Hydrogen Bond*. Oxford University Press.

Fabbiani, F. P. A., Allan, D. R., Dawson, A., David, W. I. F., McGregor, P. A., Oswald, I. D. H., Parsons, S. & Pulham, C. R. (2003). *Chem. Commun.* **24**, 3004–3005.

Hirshfeld, F. L. (1977). *Theor. Chim. Acta*, **44**, 129–138.

Jönsson, P. G. (1976). *Acta Cryst.* B**32**, 232–235.

McGregor, P. A., Allan, D. R., Parsons, S. & Pulham, C. R. (2005). *Acta Cryst.* B**61**, 449–454.

McKinnon, J. J., Spackman, M. A. & Mitchell, A. S. (2004). *Acta Cryst.* B**60**, 627–668.

Merrill, L. & Basset, W. A. (1974). *Rev. Sci. Instrum.* **45**, 290–294.

Narten, A. H. & Habenschuss, A. (1984). *J. Chem. Phys.* **80**, 3387–3391.

Oswald, I. D. H., Allan, D. R., Motherwell, S. W. D. & Parsons, S. (2005). *Acta Cryst.* B**61**, 69–79.

Peresypkina, E. V. & Blatov, V. A. (2000). *Acta Cryst.* B**56**, 501–511.

Sheldrick, G. M. (1997a). *SHELXTL*. Bruker-AXS, Madison, Wisconsin, USA.

Sheldrick, G. M. (1997b). *SHELXS97*. University of Göttingen, Germany.

Sheldrick, G. M. (1997c). *SHELXL97*. University of Göttingen, Germany.

Steiner, T. (2002). *Angew. Chem. Int. Ed. Engl.* **41**, 49–76.

Tauer, K. J. & Lipscomb, W. N. (1952). *Acta Cryst.* **5**, 606–612.

Torrie, B. H., Weng, S. X. & Powell, B. M. (1989). *Mol. Phys.* **67**, 575–581.

UWA Theoretical Chemistry (undated). *Crystal Explorer*, Version 1.0.3, http://www.theochem.uwa.edu.au/crystal_explorer.